

THE PHYSICS OF TIBETAN SINGING BOWLS

PART 2: NUMERICAL SIMULATIONS

PACS: 43.75.Kk

Inácio, Octávio¹; Henrique, Luís¹; Antunes, José²

¹ Escola Superior de Música e Artes do Espectáculo, Instituto Politécnico do Porto
Laboratório de Acústica Musical, Rua da Alegria, 503, 4000-045 Porto, Portugal
Tel: (351) 225193760, Fax: (351) 225180774
Email: Octaviolnacio@esmae-ipp.pt; LuisLeite@esmae-ipp.pt

² Instituto Tecnológico e Nuclear
Applied Dynamics Laboratory
ITN/ADL, Estrada Nacional 10, 2686-953 Sacavém Codex, Portugal
Tel: (351) 219946142, Fax: (351) 219941039, Email: jantunes@itn.mces.pt

ABSTRACT

In a companion paper we presented a modal method to simulate the dynamical responses of a Tibetan bowl under impact or rubbing excitation. In this paper we demonstrate the effectiveness of such modelling techniques with numerical simulations of bowls subjected to various playing conditions.

We start by showing the influence of the contact model parameters on the dynamical responses of impacted bowls. Then proceed to rubbing excitation, assuming time-constant values of the normal force and tangential velocity imposed to the moving *puja*. For suitable friction parameters and for adequate ranges of the normal contact force and tangential rubbing velocity of the *puja*, instability of one of the lower-frequency shell modes (usually the first one) arises, with exponential increase of the vibration amplitude until saturation by nonlinear effects.

Our simulation results highlight the existence of several motion regimes, both steady and unsteady, with either permanent or intermittent bowl/*puja* contact. Furthermore, the unstable modes spin at the angular velocity of the *puja*. As a consequence, for the listener, singing bowls behave as rotating quadropoles. The sound will always be perceived as beating phenomena, even if using perfectly symmetrical bowls. From our computations, sounds and animations have been produced, which appear to agree with qualitative experiments.

INTRODUCTION

In [1] we developed techniques for the physical modelling of Tibetan bowls, when subjected to impact, rub, or any combination of excitations. Here we will present results of a series of exploratory numerical simulations, for both impacted and rubbed bowls, which both demonstrate the effectiveness of the proposed computational techniques and highlight the main features of the physics of singing bowls.

We discuss extensively the influence of the contact/friction parameters – as well as the influence of the normal contact force F_N and of the tangential velocity V_T of the exciter – on the produced sounds. From our computations, sounds and animations have been produced. Many aspects of the bowl responses highlighted in our simulations have been observed in preliminary qualitative experiments.

NUMERICAL SIMULATIONS

The numerical simulations presented here are based on the modal data of Bowl 2 (with rim diameter of 152 mm, a total mass of 563 g and a fundamental frequency of 314 Hz), which were identified in Part 1 (see Figure 1 in [1]). The *puja* is modeled as a simple mass of 20 g, moving at tangential velocity V_T , and subjected to an external normal force F_N as well as to the bowl/*puja* nonlinear interaction force.

We explore a significant range of rubbing parameters: $F_N = 1 \sim 9$ N and $V_T = 0.1 \sim 0.5$ m/s, which encompass the usual playing conditions, although calculations were made also using impact excitation only. For clarity, the normal force and tangential velocity will be assumed time-constant, in the present simulations. However, nothing would prevent us from imposing any time-varying functions $F_N(t)$ and $V_T(t)$, or even – as musicians would do – to couple the generation of $F_N(t)$ and $V_T(t)$ with the nonlinear bowl/*puja* dynamical simulation, through well-designed *control strategies*, in order to achieve a suitable response regime.

The contact model used in all rubbing simulations has a contact stiffness of $K_c = 10^6$ N/m and a contact dissipation of $C_c = 50$ Ns/m, which appear adequate for the present system. However, concerning impact simulations, contact parameters ten times higher and lower were also explored. The friction parameters used in numerical simulations of rubbed bowls are $m_\xi = 0.4$, $m_\eta = 0.2$ and $C = 10$ (see Figure 5 in [1]). No effort, at this stage, was made to explore other friction laws, however the parameters used tentatively here seem realistic enough.

Seven mode pairs were used to describe the dynamics of Bowl 2 (see Table 1 and Figure 4 in [1]). An average value of 0.005% was used for all modal damping coefficients. As discussed in Part 1, assuming a perfectly symmetrical bowl, simulations were performed using identical frequencies for each mode-pair ($w_n^A = w_n^B$). However, a few computations were also performed for less-than-perfect systems, asymmetry being then modelled introducing a difference (or “split”) Δw_n between the frequencies of each mode pair. In order to cope with the large settling times that arise with singing bowls, 20 seconds of computed data were generated (enough to accommodate transients for all rubbing conditions), at a sampling frequency of 22050 Hz.

Impact Responses

Figures 1(a-c) display the simulated responses of a perfectly symmetrical bowl to an impact excitation ($V_N(t_0) = 1$ m/s), assuming different values for the contact model parameters. The time-histories of the response displacements pertain to the impact location. The spectrograms are based on the corresponding velocity responses. Typically, as the contact stiffness increases from 10^5 N/m to 10^7 N/m, higher-order modes become increasingly excited and resonate longer. The corresponding simulated sounds become progressively brighter, denoting the “metallic” bell-like tone which is clearly heard when impacting real bowls using wood or metal *pujas*.

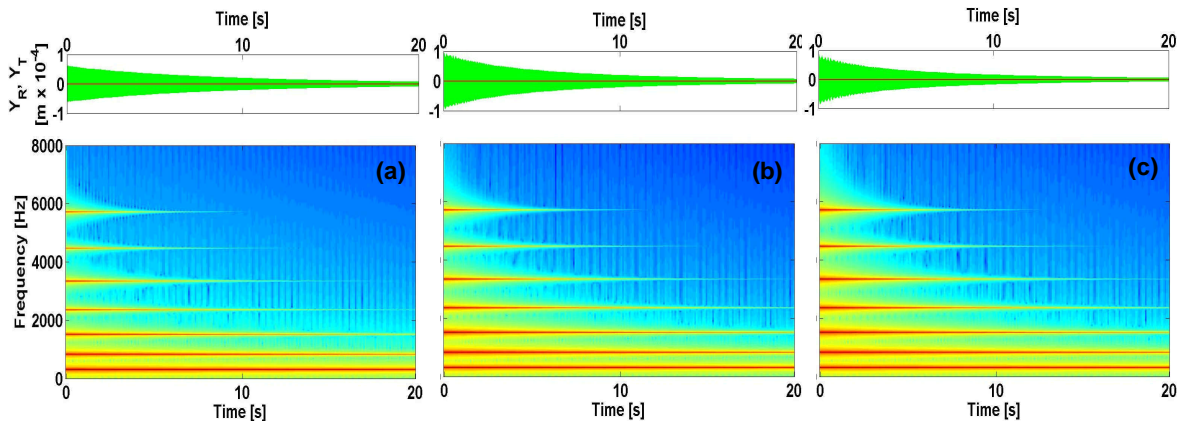


Figure 1 – Displacement time histories (top) and spectrograms (bottom) of the response of Bowl 2 to impact excitation with different values of the bowl/*puja* contact stiffness: (a) 10^5 N/m ; (b) 10^6 N/m ; (c) 10^7 N/m

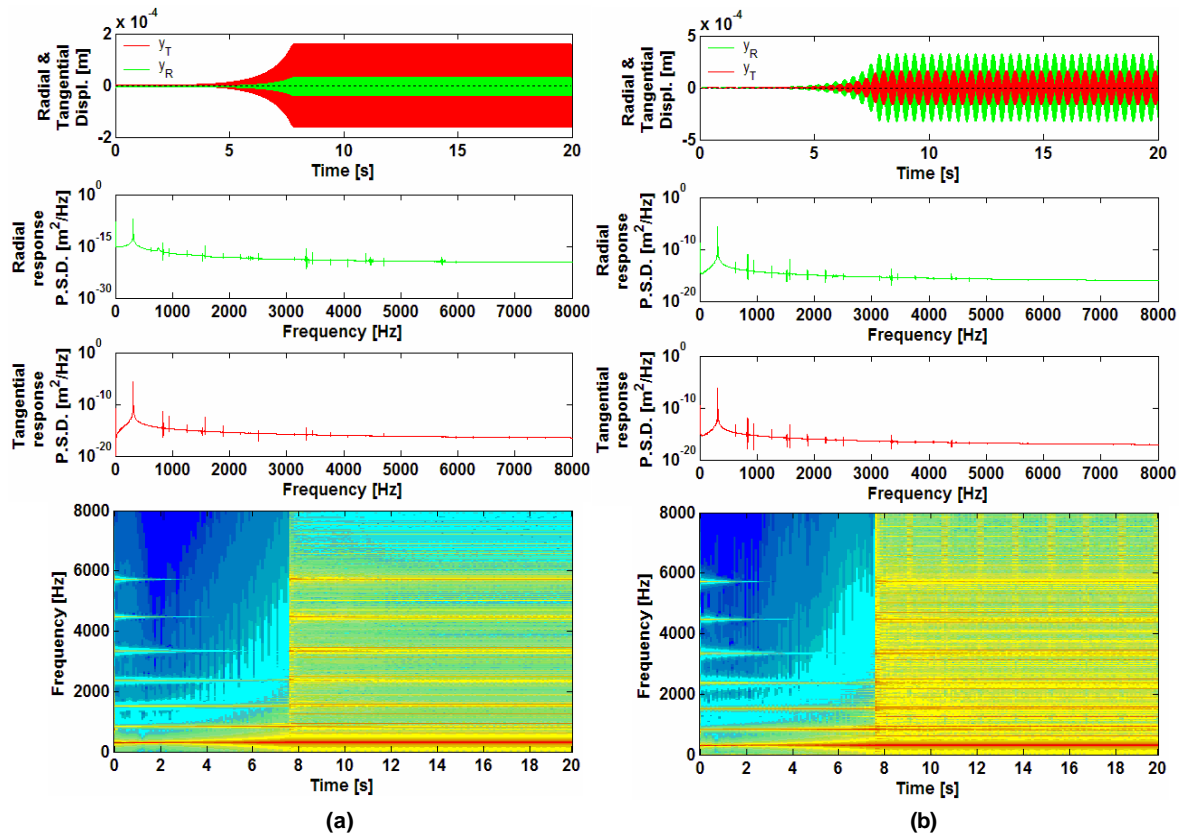


Figure 2 – Time-histories, spectra and spectrograms of the dynamical response of Bowl 2 to friction excitation when $F_N = 3 \text{ N}$, $V_T = 0.3 \text{ m/s}$: (a) at the bowl/puja travelling contact point; (b) at a fixed point of the bowls rim

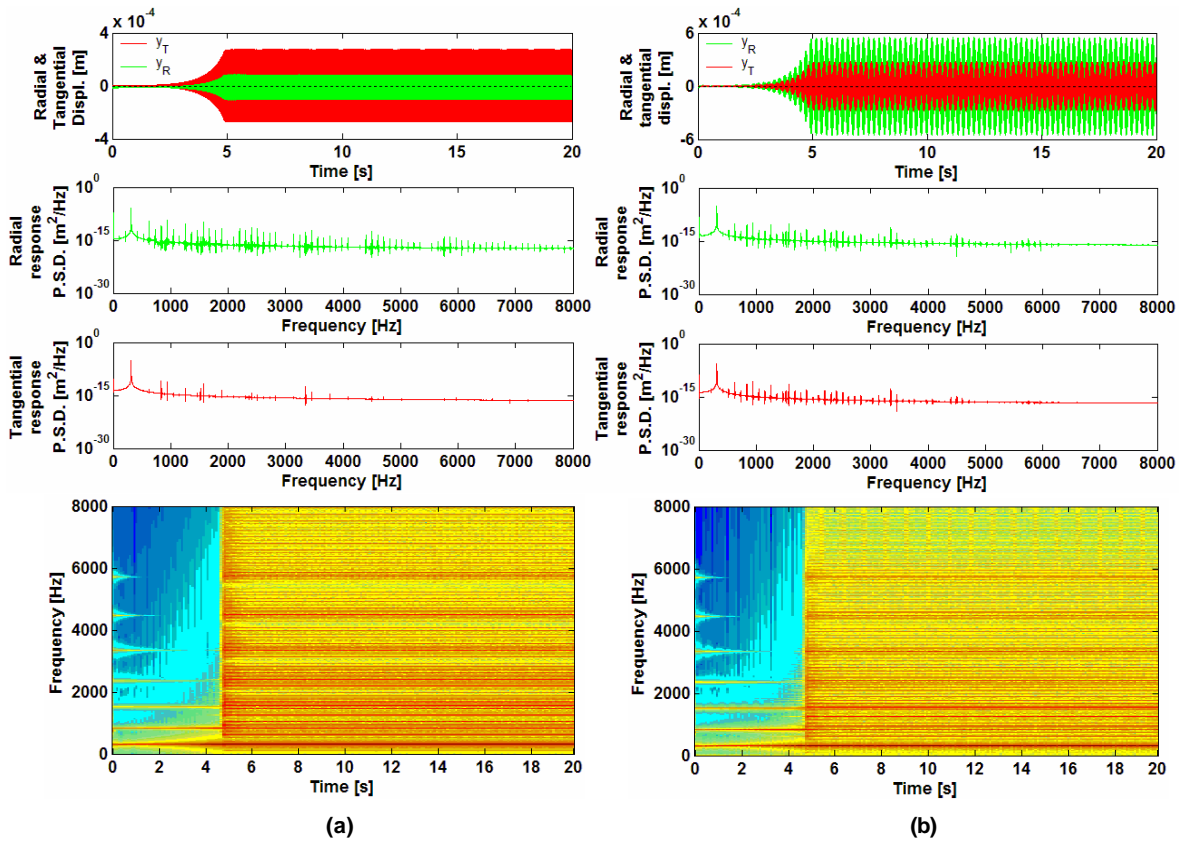


Figure 3 – Time-histories, spectra and spectrograms of the dynamical response of Bowl 2 to friction excitation when $F_N = 7 \text{ N}$, $V_T = 0.5 \text{ m/s}$: (a) at the bowl/puja travelling contact point; (b) at a fixed point of the bowls rim

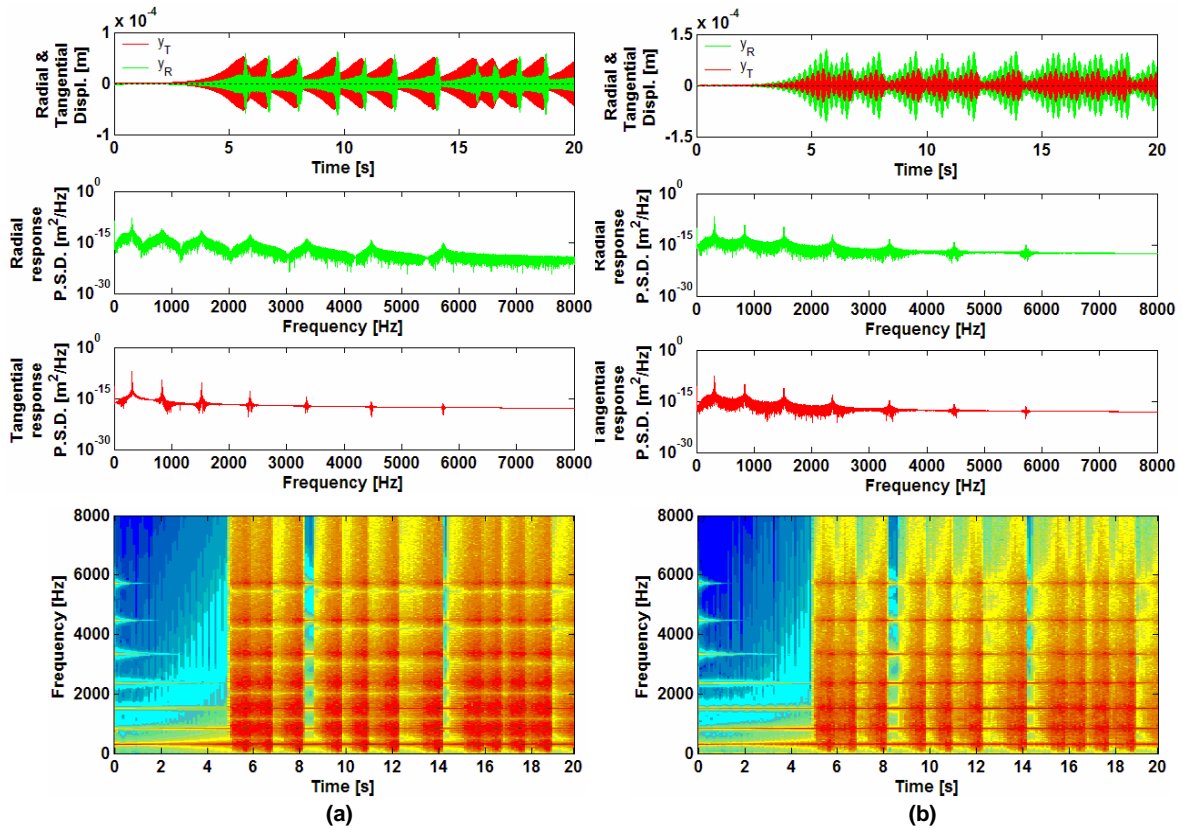


Figure 4 – Time-histories, spectra and spectrograms of the dynamical response of Bowl 2 to friction excitation when $F_N = 1$ N, $V_T = 0.5$ m/s : (a) at the bowl/puja travelling contact point; (b) at a fixed point of the bowls rim

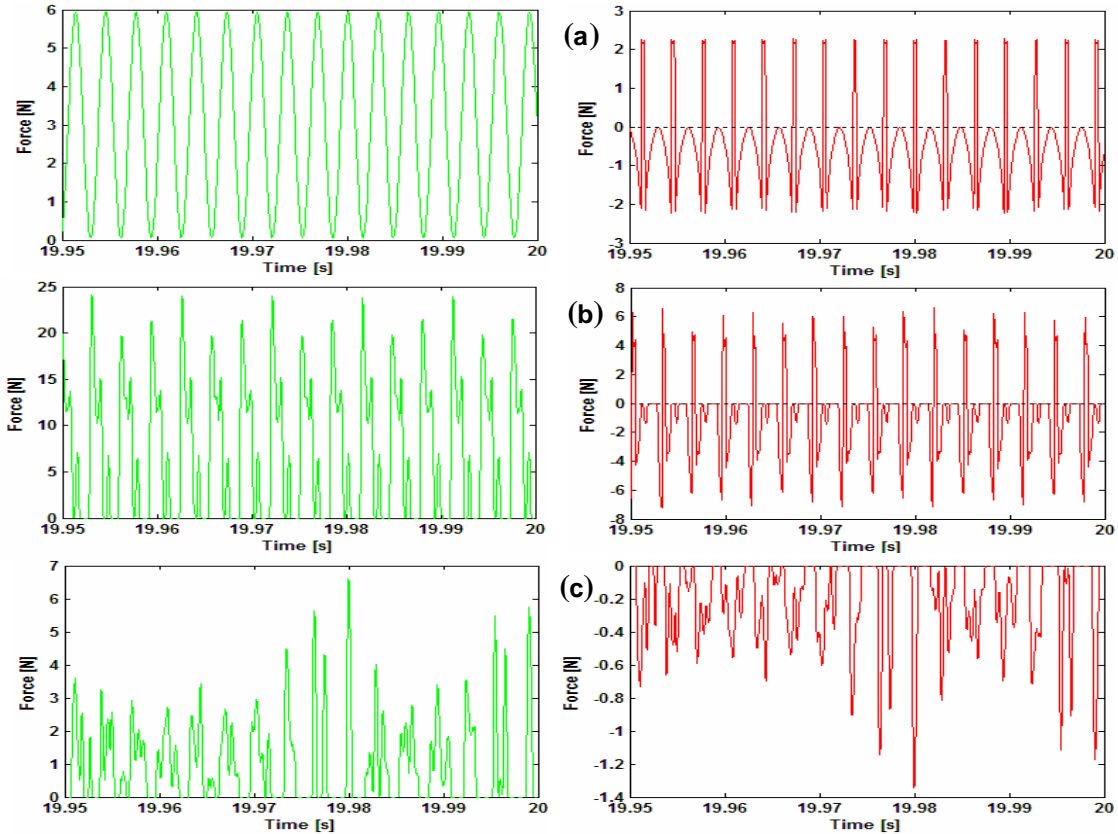


Figure 5 – Radial (green) and tangential (red) interaction forces between the bowl and the travelling puja: (a) $F_N = 3$ N, $V_T = 0.3$ m/s; (b) $F_N = 7$ N, $V_T = 0.5$ m/s; (c) $F_N = 1$ N, $V_T = 0.5$ m/s

Friction-Excited Responses

Figure 2 shows the results obtained when rubbing a perfectly symmetrical bowl near the rim, using fairly standard rubbing conditions: $F_N = 3$ N and $V_T = 0.3$ m/s. The plots shown pertain to the following response locations: (a) the travelling contact point between the bowl and the *puja*; (b) a fixed point in the bowl's rim. Depicted are the time-histories and corresponding spectra of the radial (green) and tangential (red) displacement responses, as well as the spectrograms of the radial velocity responses.

As can be seen, an instability of the first "elastic" shell mode (with 4 azimuthal nodes) arises, with an exponential increase of the vibration amplitude until saturation by nonlinear effects is reached (at about 7.5 s), after which the self-excited vibratory motion of the bowl becomes steady. The response spectra show that most of the energy lays in the first mode, the others being marginally excited. Notice the dramatic differences between the responses at the travelling contact point and at a fixed location. At the moving contact point, the motion amplitude does not fluctuate and the tangential component of the motion is significantly higher than the radial component. On the contrary, at a fixed location, the motion amplitude fluctuates at a frequency which can be identified as being four times the spinning frequency of the *puja*: $\Omega_{fluct} = 4\Omega_{puja} = 4(2V_T/f)$. Furthermore, at a fixed location, the amplitude of the radial motion component is higher than the tangential component.

The animations of the bowl and *puja* motions enable an interpretation of these results. After synchronisation of the self-excited regime, the combined responses of the first mode-pair result in a vibratory motion according to the 4-node modeshape, which however spins, "following" the revolving *puja*. Furthermore, synchronisation settles with the *puja* interacting near a node of the radial component, corresponding to an anti-nodal region of the tangential component – see Figure 4 and Equations (5,6) in [1]. In retrospect, this appears to make sense – indeed, because of the friction excitation mechanism in singing bowls, the system modes self-organize in such way that a high *tangential* motion-component will arise at the contact point, where energy is inputted.

At any fixed location, a transducer will "see" the vibratory response of the bowl modulated in amplitude, as the $2j$ alternate nodal and anti-nodal regions of the "singing" modeshape revolve. For a listener, the rubbed bowl behaves as a spinning quadropole – or, in general, a $2j$ -pole (depending on the self-excited mode j) – and the radiated sound will always be perceived with beating phenomena, even for a perfectly symmetrical bowl. Following the previous remarks, the out-of-phase envelope modulations of the radial and tangential motion components at a fixed location, as well as their amplitudes, can be easily understood. Indeed, all necessary insight stems from Equations (5,6) and the first plot of Figure 4, in Part 1.

It should be noted that our results basically support the qualitative remarks provided by Rossing, when discussing friction-excited musical glass-instruments (see [2], pp. 185-187 – the only reference, to our knowledge, where some attention has been paid to these issues). However, his main point "*The location of the maximum motion follows the moving finger around the glass*" may now be further clarified: the "maximum motion" following the exciter should refer in fact to the maximum *tangential* motion component (and not the radial component, as might be assumed).

Before leaving this example, notice in Figure 5(a) the behaviour of the radial and tangential components of the bowl/*puja* contact force, on several cycles of the steady motion. The radial component oscillates between almost zero and the double of the value F_N imposed to the *puja*, and contact is never disrupted. The plot of the friction force shows that the bowl/*puja* interface is sliding during most of the time. This behaviour is quite similar to what we observed in simulations of bowed bars, and is in clear contrast to bowed strings, which adhere to the bow during most of the time – see [3], for a detailed discussion. The fact that sticking only occurs during a short fraction of the motion, justifies in a way the simplified friction model presented in Part 1, which has been used for the present computations.

Figure 3 shows the results for a slightly different regime, corresponding to rubbing conditions: $F_N = 7$ N and $V_T = 0.7$ m/s. The transient duration is smaller than in the previous case (about 5 s). Also, because of the higher tangential *puja* velocity, beating of the vibratory response at the fixed location also displays a higher frequency. This motion regime seems qualitatively similar to the previous example, however notice that the response spectra display more energy at higher frequencies, and that is because the contact between the exciter and the bowl is periodically disrupted, as shown in the contact force plots of Figure 5(b). One can see that, during about 25% of the time, the contact force is zero. Also, because of moderate impacting, the maxima of the radial component reach almost $3F_N$. Both the radial and friction force components are much less regular than in the previous example, but this does not prevent the motion from being nearly-periodic.

Figure 4 shows a quite different behaviour, when $F_N = 1$ N and $V_T = 0.5$ m/s. Here, a steady motion is never reached, as the bowl/*puja* contact is disrupted whenever the vibration amplitude reaches a certain level. As shown in Figure 5 (c), severe chaotic impacting arises (the amplitude of the radial component reaches almost $7F_N$), which breaks the mechanism of energy transfer, leading to a sudden decrease of the motion amplitude. Then, the motion build-up starts again until the saturation level is reached, and so on. As can be expected, this intermittent response regime results in curious sounds, which interplay the aerial characteristics of “singing” with a distinct “ringing” response due to chaotic chattering. Anyone who ever attempted to play a Tibetan bowl is well aware of this sonorous saturation effect, which can be musically interesting, or a vicious nuisance, depending on the context.

To get a clearer picture of the global dynamics of this system, Figures 6 and 7 present the domains covered by the three basic motion regimes (typified in Figures 2-4), as a function of F_N and V_T : (1) Steady self-excited vibration with permanent contact between the *puja* and the bowl (green data); (2) Steady self-excited vibrations with periodic contact disruption (yellow data); (3) Unsteady self-excited vibrations with intermittent amplitude increasing followed by attenuation after chaotic chattering (orange data). Note that, under different conditions, the self-excitation of a different mode may be triggered – for instance, by starting the vibration with an impact followed by rubbing. However, such procedures and results will not be discussed here.

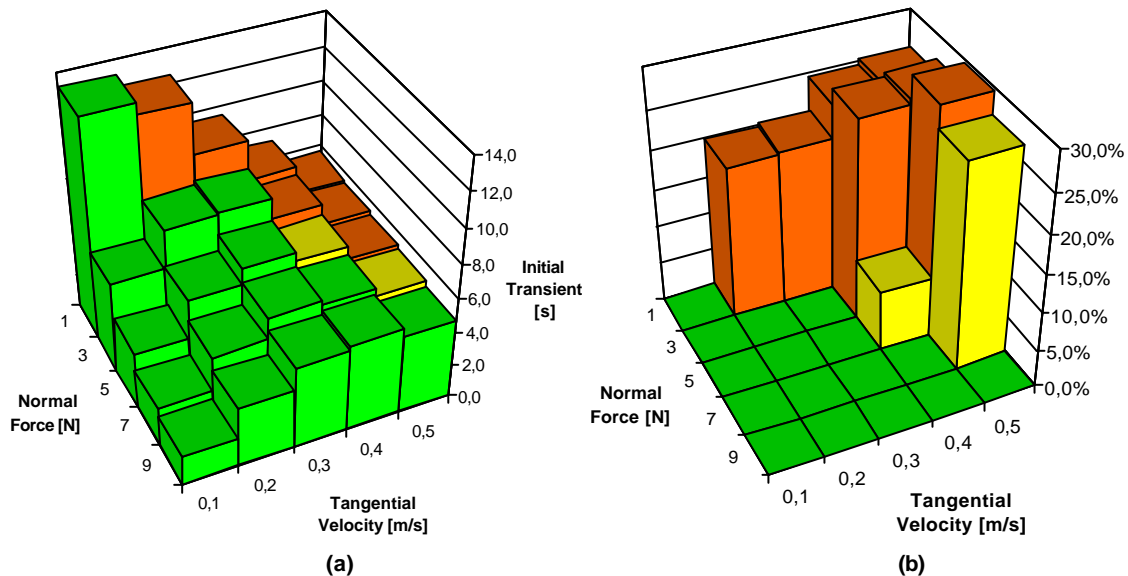


Figure 6 – (a) Initial transient duration and (b) percentage of time with no bowl/*puja* contact, as a function of F_N and V_T

Figure 6(a) shows how the initial transient duration depends on F_N and V_T . In every case, transients are shorter for increasing normal forces, though such dependence becomes almost negligible at higher tangential velocities. At constant normal force, the influence of V_T strongly depends on the motion regime. Figure 6 (b) shows the fraction of time with motion disruption. It

is obviously zero for regime (1), and growing up to 30 % at very high excitation velocities. It is clear that the ‘finging’ regime (3) is more prone to arise at low excitation forces and higher velocities.

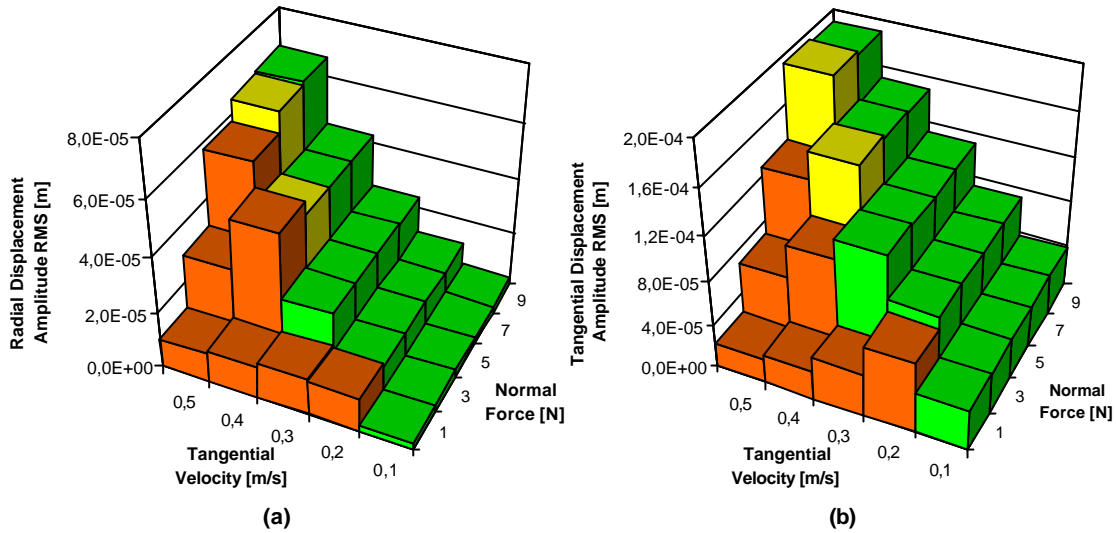


Figure 7 – (a) Radial and (b) Tangential displacement amplitude (RMS) at the bowl/puja travelling contact point, as a function of F_N and V_T

Figures 7(a) and (b) show the root-mean-square vibratory amplitudes *at the traveling contact point*, as a function of F_N and V_T . Notice that the levels of the radial components are much lower than the corresponding levels of the tangential component, in agreement with the previous comments. These plots show some dependence of the vibratory level on the response regime. Overall, the vibration amplitude increases with V_T for regime (1) and decreases for regime (3). On the other hand, it is almost independent of F_N for regime (1), while it increases with F_N for regime (3).

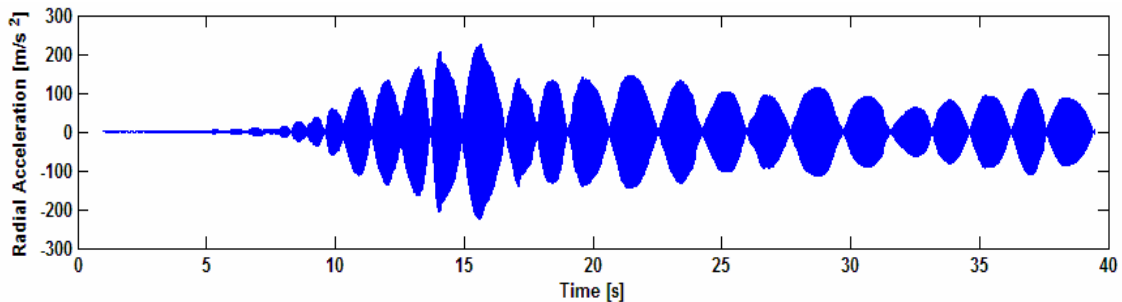


Figure 8 – Experimental measurement of the radial acceleration at a point of the bowl rim due to friction excitation by a rubber puja

The last item in this section, Figure 8, presents an experimental acceleration response of a rubbed bowl, under uncontrolled (but typical playing) conditions. This plots many of the features highlighted by the numerical simulations.

Non-Symmetrical Bowls

Figures 9(a) and (b) enable a comparison between the impact responses of perfectly symmetrical and a non-symmetrical bowls. Here, the lack of symmetry has been simulated by introducing a frequency split of 2% between the frequencies of each mode-pair (e.g. $\Delta w_n = 0.02 w_n$), all other aspects remaining identical – such crude approach is adequate for illustration purposes.

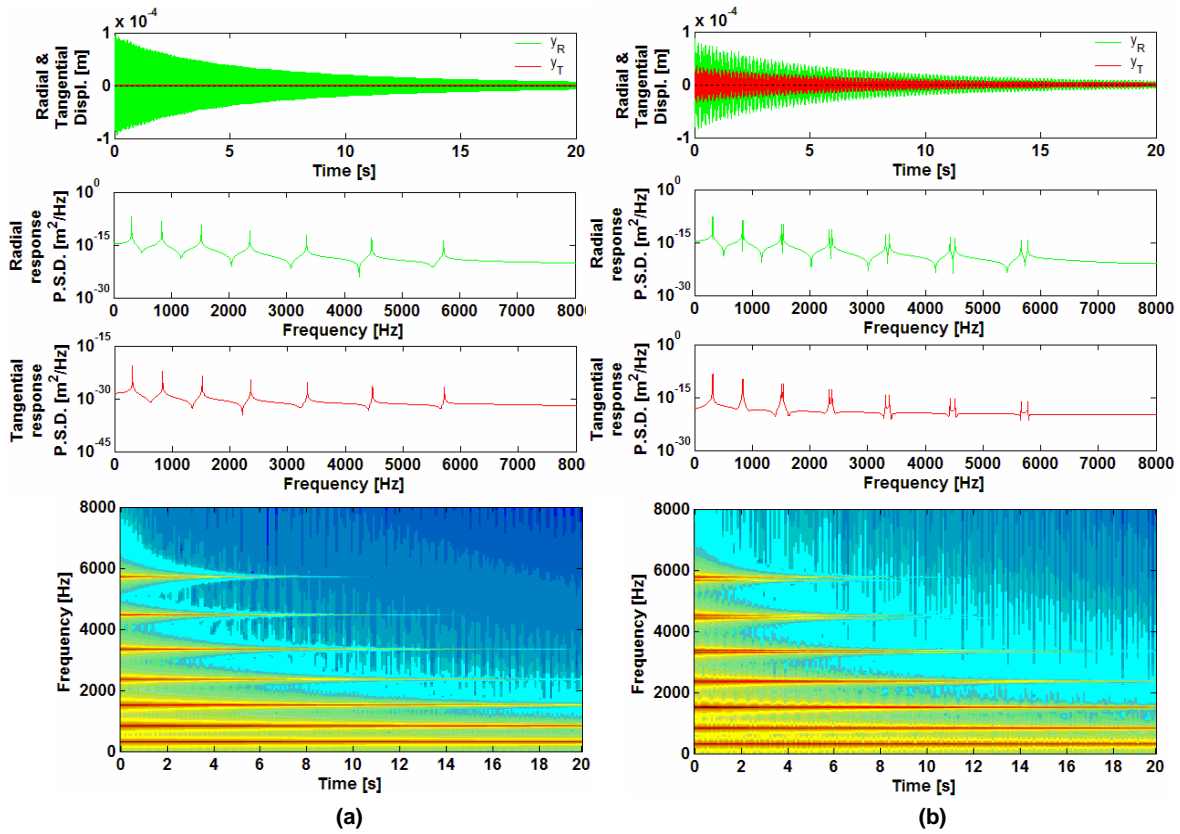


Figure 9 – Dynamical responses of an impacted bowl, at the impact location:
 (a) Axi-symmetrical bowl (0% frequency split); (b) Non-symmetrical bowl with 2% frequency split

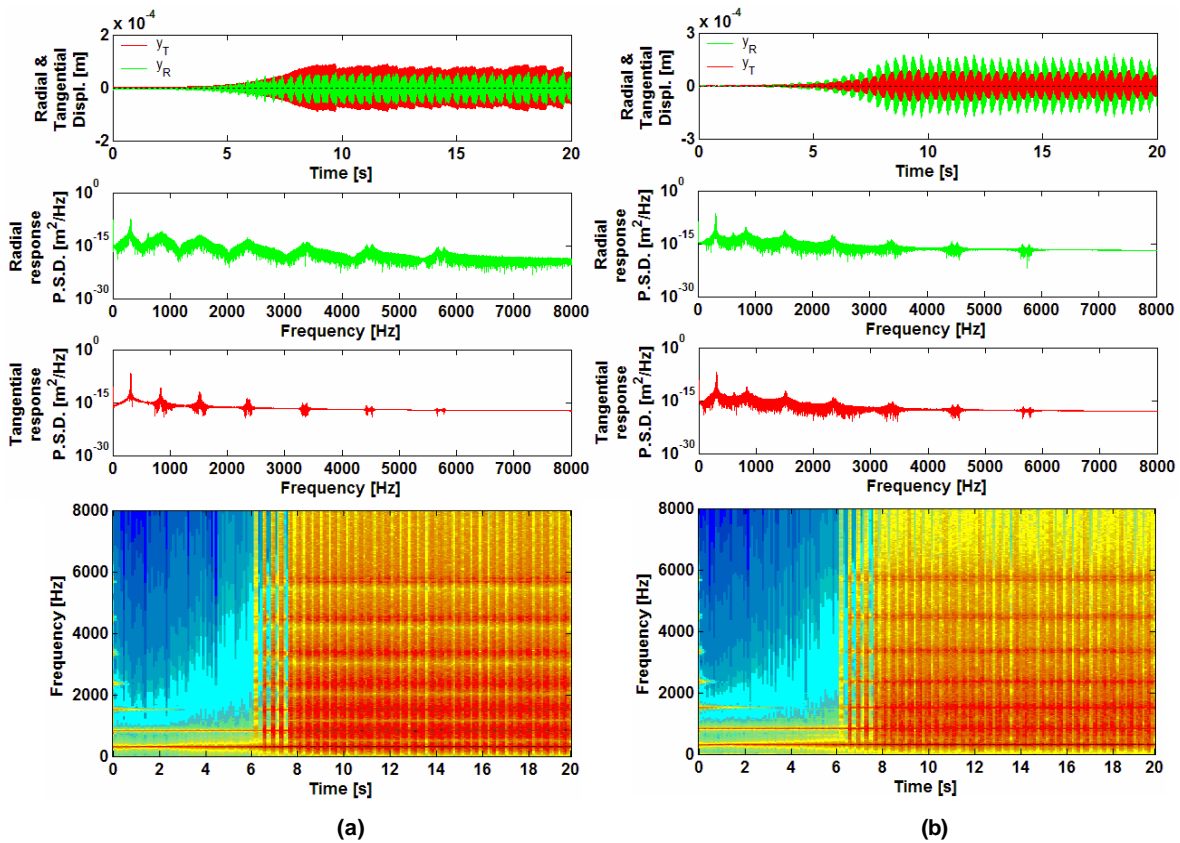


Figure 10 – Dynamical response of a rubbed bowl with 2% frequency split when $F_N = 3$ N, $V_T = 0.3$ m/s:
 (a) at the bowl/puja travelling contact point; (b) at a fixed point of the bowls rim

Notice that the symmetrical bowl only displays radial motion *at the impact point* (as it should), while the unsymmetrical bowl displays both radial and tangential motion components due to the different propagation velocities of the travelling waves excited. On the other hand, one can notice in the response spectra of the unsymmetrical system the frequency-split of the various mode-pairs. This leads to beating of the vibratory response, as clearly seen on the corresponding spectrogram.

Figure 10 shows the self-excited response of the symmetrical bowl, when rubbed at $F_N = 3$ N and $V_T = 0.3$ m/s. Notice that sound beating due to the spinning of the response modeshape dominates, when compared to effect of modal frequency-split. Interestingly, the slight change in the modal frequencies was enough to modify the nature of the self-excited regime, which went from type (1) to type (3). This fact shows the difficulties in mastering these apparently simple instruments.

CONCLUSIONS

The numerical simulations presented in this paper show some light on the sound-producing mechanisms of Tibetan singing bowls. Both impact and friction excitations have been addressed, as well as perfectly-symmetrical and less-than-perfect bowls (a very common occurrence). For suitable friction parameters and for adequate ranges of the normal contact force F_N and tangential rubbing velocity V_T of the *puja*, instability of a shell mode (typically the first "elastic" mode, with 4 azimuthal nodes) arises, with an exponential increase of the vibration amplitude followed by saturation due to nonlinear effects.

Because of the intimate coupling between the radial and tangential shell motions, the effective bowl/*puja* contact force is not constant, but oscillates. After vibratory motions settle, the excitation point tends to locate near a nodal region of the *radial* motion of the unstable mode, which corresponds to an anti-nodal region of the friction-excited *tangential* motion. This means that unstable modes spin at the same angular velocity of the *puja*. As a consequence, for the listener, sounds will always be perceived with beating phenomena. However, for a perfectly symmetrical bowl, no beating at all is generated at the moving excitation point.

Typically, the transient duration increases with V_T and decreases for higher values of F_N . The way vibratory amplitudes depend on V_T and F_N changes for different response regimes. Three basic motion regimes were obtained in the present computations, depending on F_N and V_T : (1) Steady self-excited vibration with permanent contact between the *puja* and the bowl; (2) Steady self-excited vibrations with periodic contact disruption; (3) Unsteady self-excited vibrations with intermittent amplitude increasing followed by attenuation after chaotic chattering.

The first motion regime offers the "purest" bowl singing. Our results suggest that higher values of F_N should enable a better control of the produced sounds, as they lead to shorter transients and also render the system less prone to chattering.

REFERENCES

- [1] O. Inácio, L. Henrique, J. Antunes, "The Physics of Singing Bowls – Part 1: Physical Modelling", 34^o Congreso Nacional de Acústica y Encuentro Ibérico de Acústica (TecniAcustica 2003), Bilbao, España (2003).
- [2] T. D. Rossing, "Science of Percussion Instruments", World Scientific, New Jersey, USA (2000).
- [3] O. Inácio, L. Henrique, J. Antunes, "Nonlinear Dynamics and Playability of Bowed Instruments: From the Bowed String to the Bowed Bar", Proceedings of the Eleventh International Conference on Computational Methods and Experimental Measurements (CMEM 2003), Halkidiki, Greece (2003).